

# Stable monolayer honeycomb like structures of RuX<sub>2</sub> (X=S, Se)

Fatih Ersan,<sup>1</sup> Seymur Cahangirov,<sup>2</sup> Gökhan Gökoğlu,<sup>3</sup> Angel Rubio,<sup>4,5,\*</sup> and Ethem Aktürk<sup>1,6,†</sup>

<sup>1</sup>*Department of Physics, Adnan Menderes University, Aydin 09010, Turkey*

<sup>2</sup>*UNAM-Institute of Materials Science and Nanotechnology, Bilkent University, Ankara 06800, Turkey*

<sup>3</sup>*Department of Physics, Karabük University, 78050 Karabük, Turkey*

<sup>4</sup>*Max Planck Institute for the Structure and Dynamics of Matter,  
Luruper Chaussee 149, 22761 Hamburg, Germany*

<sup>5</sup>*Nano-Bio Spectroscopy Group and ETSF, Dpto. Fisica de Materiales,  
Universidad del País Vasco, 20018 San Sebastián, Spain*

<sup>6</sup>*Nanotechnology Application and Research Center,  
Adnan Menderes University, Aydin 09010, Turkey*

(Dated: September 21, 2016)

PACS numbers: 31.15.A-, 71.15.Mb, 73.20.-r, 81.05.Zx

## I. BULK RUX<sub>2</sub>

For the sake of comparison, we optimize the bulk forms of RuX<sub>2</sub> structures. The obtained structural and electronic parameters are presented in Table 1. The structural parameters of pyrite RuX<sub>2</sub> systems are in excellent agreement with the experimental results. We find E<sub>g</sub> values, the energy gaps of bulk RuX<sub>2</sub>, as the half of the experimental results due to standard PBE calculations, but their band characteristics are the same with the literature as illustrated in Fig.1.

## II. T'-RUX<sub>2</sub>

Kuc et al. present that the estimation of electronic properties of TMDs within PBE0 or B3LYP give much worse results than HSE06 calculations<sup>2,3</sup>. Since the experimental results of T'-RuX<sub>2</sub> structures are not available, we also calculate the bandgap of T'-RuX<sub>2</sub> structures by using different DFT+HF methods. Fig.2 illustrates the obtained band dispersions of T'-RuX<sub>2</sub> structures by B3LYP and PBE0 calculations. The band structures have similar characteristics with different bandgap values.

In Table 2, we present some additional crystallographic parameters including bond lengths and angles of T and T' forms of 2D-RuX<sub>2</sub> structures.

Fig.3 displays the thermodynamic variables of T'-RuX<sub>2</sub> structures as a function of the temperature in the range of 0-1000 K. All of these functions are extracted from the calculated phonon dispersion relations at zero pressure by using PHONOPY programme<sup>4</sup>. As can be seen in Fig.3, the thermodynamic variables show dramatic changes specially at low temperatures below 200 K. For instance, while T'-RuX<sub>2</sub> has almost fixed free energy below 100 K with low entropic contributions, it goes to negative values with increasing temperature. Entropy of T'-RuX<sub>2</sub> also increases with temperature as expected. And finally, we present volumetric specific heat C<sub>v</sub> of T'-RuX<sub>2</sub>. It is seen that the heat capacity depends on

temperature at T<400 K and C<sub>v</sub> goes to zero while the temperature goes to zero in accordance with the third law of thermodynamics. At high temperatures, C<sub>v</sub> tends to the Dulong-Petit limit, especially over the 400 K all of the T'-RuX<sub>2</sub> heat capacities have same values.

## III. OPTICAL PROPERTIES

From the dynamical dielectric response functions  $\varepsilon(\omega)$ , the main optical spectra; such as reflectivity R( $\omega$ ), absorption coefficient  $\alpha(\omega)$ , energy loss spectrum L( $\omega$ ) can be obtained. We calculate them by using the following equations;

$$R(\omega) = \left| \frac{\sqrt{\varepsilon(\omega)} - 1}{\sqrt{\varepsilon(\omega)} + 1} \right|^2 \quad (1)$$

$$\alpha(\omega) = (\sqrt{2})\omega[\sqrt{\varepsilon_1(\omega)^2 + \varepsilon_2(\omega)^2} - \varepsilon_1(\omega)]^{1/2} \quad (2)$$

$$L(\omega) = \varepsilon_2(\omega)/[\varepsilon_1(\omega)^2 + \varepsilon_2(\omega)^2] \quad (3)$$

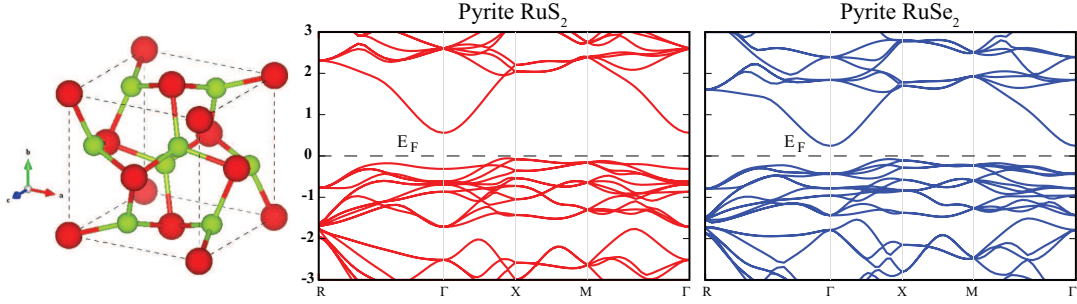


FIG. 1. Bulk pyrite structure of  $\text{RuX}_2$  ( $\text{X}=\text{S}, \text{Se}$ ) and electronic band dispersions.

TABLE I. The obtained parameters for bulk  $\text{RuX}_2$ ; lattice constants [experimental<sup>1</sup>], Ru-Ru and Ru-X distances, band gap energies [experimental<sup>1</sup>].

System	Structure	lattice ( $\text{\AA}$ )	$d_{\text{Ru}-\text{Ru}}$ ( $\text{\AA}$ )	$d_{\text{Ru}-\text{X}}$ ( $\text{\AA}$ )	$E_g$ (eV)
$a=b=c$					
$\text{RuS}_2$	Pyrite	5.596 [5.609]	3.957	2.343	0.62 [1.22]
$\text{RuSe}_2$	Pyrite	5.942 [5.934]	4.202	2.427	0.33 [0.76]

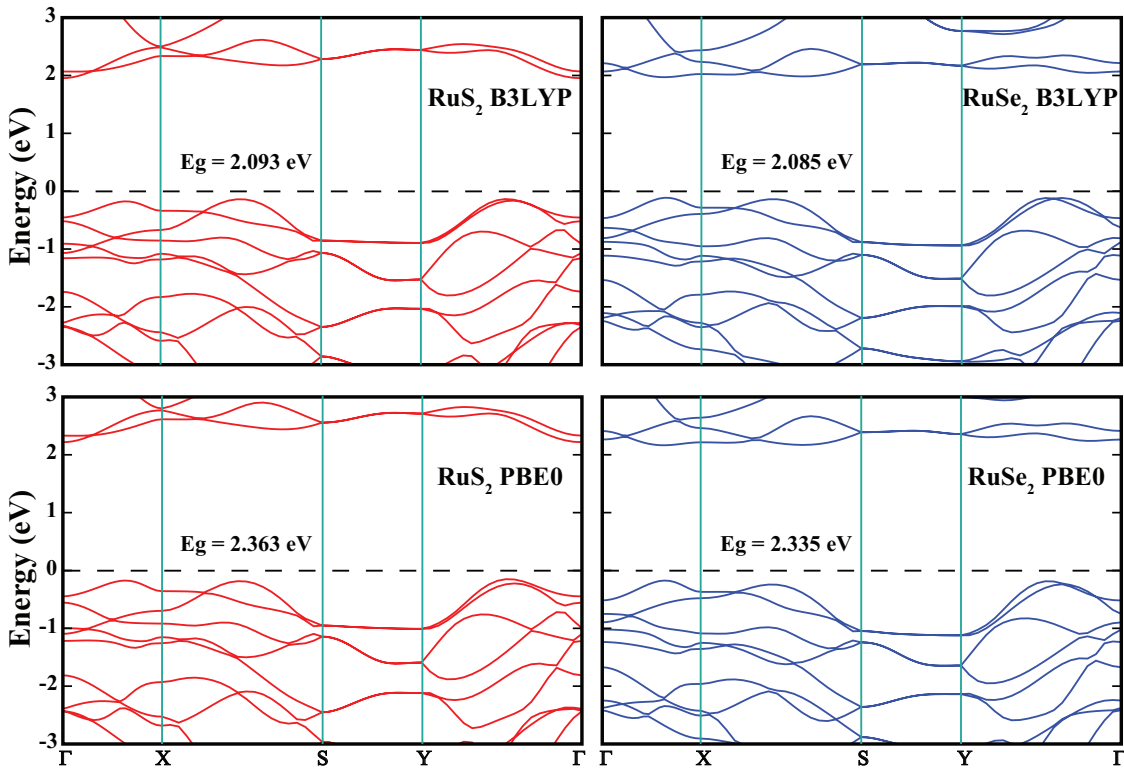


FIG. 2. Band dispersions of  $T'$ - $\text{RuX}_2$  structures according to B3LYP and PBE0 calculations.

TABLE II. The equilibrium optimized structural parameters of 2D  $\text{RuX}_2$  ( $\text{X}=\text{S}, \text{Se}$ ) systems in  $T$  and  $T'$  forms: lattice constants, Ru-Ru and Ru-X distances, bond angles.

System	Lattice ( $\text{\AA}$ )	$d_{\text{Ru}-\text{Ru}}$ ( $\text{\AA}$ )	$d_{\text{Ru}-\text{X}}$ ( $\text{\AA}$ )	$\Theta$ (deg)
$T\text{-RuS}_2$	$a=b=3.338$	$\text{Ru-Ru}=3.338$	$\text{Ru-S}=2.390$	$\text{SRuS}=91.48$
$T\text{-RuSe}_2$	$a=b=3.475$	$\text{Ru-Ru}=3.475$	$\text{Ru-Se}=2.515$	$\text{SeRuSe}=92.66$
$T'\text{-RuS}_2$	$a=5.561$ $b=3.450$	$\text{Ru}_1\text{-Ru}_2=2.829$ $\text{Ru}_2\text{-S}_2=2.384$ $\text{Ru}_1\text{-S}_1=2.384$ $\text{Ru}_2\text{-S}_3=2.381$ $\text{Ru}_1\text{-S}_2=2.258$	$\text{Ru}_1\text{Ru}_2\text{Ru}_1=75.15$ $\text{Ru}_1\text{S}_1\text{Ru}_1=92.68$ $\text{Ru}_1\text{S}_2\text{Ru}_2=75.03$	
$T'\text{-RuSe}_2$	$a=5.789$ $b=3.597$	$\text{Ru}_1\text{-Ru}_2=2.910$ $\text{Ru}_2\text{-Se}_2=2.506$ $\text{Ru}_1\text{-Se}_1=2.506$ $\text{Ru}_2\text{-Se}_3=2.513$ $\text{Ru}_1\text{Se}_2\text{Ru}_2=73.02$ $\text{Ru}_1\text{-Se}_2=2.382$	$\text{Ru}_1\text{Ru}_2\text{Ru}_1=76.35$ $\text{Ru}_1\text{Se}_1\text{Ru}_1=91.75$ $\text{Ru}_1\text{Se}_2\text{Ru}_2=73.02$	

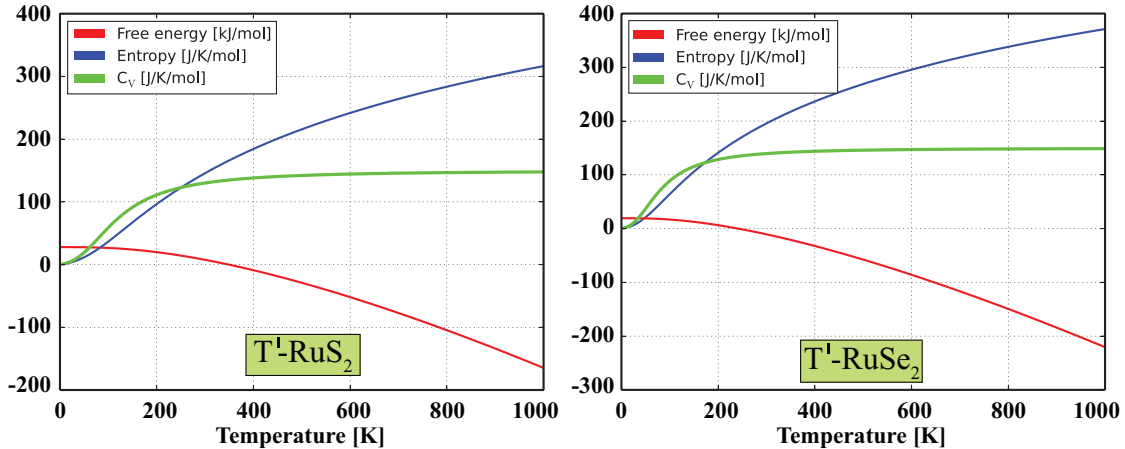


FIG. 3. Thermodynamic properties as a function of temperature of  $T'$  structures of  $\text{RuS}_2$  and  $\text{RuSe}_2$  systems.

TABLE III. Calculated Born-effective-charge tensor elements ( $Z_{ij}$ ) for the constituents of  $T'$ -RuS<sub>2</sub> structures.

	$Z_X$	$Z_Y$	$Z_Z$
Ru1	$Z_X$	-1.46469	0.00000
	$Z_Y$	-0.00085	-2.96063
	$Z_Z$	0.04141	0.00000
	$Z_X$	$Z_Y$	$Z_Z$
Ru2	$Z_X$	-1.46589	0.00000
	$Z_Y$	0.00085	-2.96063
	$Z_Z$	0.04152	0.00000
	$Z_X$	$Z_Y$	$Z_Z$
S1	$Z_X$	0.79368	0.00000
	$Z_Y$	-0.00102	1.64258
	$Z_Z$	-0.00914	0.00000
	$Z_X$	$Z_Y$	$Z_Z$
S2	$Z_X$	0.67275	0.00000
	$Z_Y$	0.00041	1.31798
	$Z_Z$	-0.03193	0.00000
	$Z_X$	$Z_Y$	$Z_Z$
S3	$Z_X$	0.67224	0.00000
	$Z_Y$	-0.00041	1.31798
	$Z_Z$	-0.03178	0.00000
	$Z_X$	$Z_Y$	$Z_Z$
S4	$Z_X$	0.79478	0.00000
	$Z_Y$	0.00102	1.64258
	$Z_Z$	-0.01010	0.00000

TABLE IV. Calculated Born-effective-charge tensor elements ( $Z_{ij}$ ) for the constituents of  $T'$ -RuSe<sub>2</sub> structures.

	$Z_X$	$Z_Y$	$Z_Z$
Ru1	$Z_X$	-2.60505	0.00000
	$Z_Y$	-0.00179	-3.24731
	$Z_Z$	0.04830	0.00000
	$Z_X$	$Z_Y$	$Z_Z$
Ru2	$Z_X$	-2.60506	0.00000
	$Z_Y$	0.00179	-3.24731
	$Z_Z$	0.04816	0.00000
	$Z_X$	$Z_Y$	$Z_Z$
Se1	$Z_X$	0.97291	0.00000
	$Z_Y$	-0.00144	1.58367
	$Z_Z$	-0.01626	0.00000
	$Z_X$	$Z_Y$	$Z_Z$
Se2	$Z_X$	1.63268	0.00000
	$Z_Y$	0.00049	1.66368
	$Z_Z$	-0.03160	0.00000
	$Z_X$	$Z_Y$	$Z_Z$
Se3	$Z_X$	1.63156	0.00000
	$Z_Y$	-0.00049	1.66368
	$Z_Z$	-0.03053	0.00000
	$Z_X$	$Z_Y$	$Z_Z$
Se4	$Z_X$	0.97468	0.00000
	$Z_Y$	0.00144	1.58367
	$Z_Z$	-0.01741	0.00000

---

\* angel.rubio@ehu.es

† ethem.akturk@adu.edu.tr

<sup>1</sup> H.P. Vaterlaus, R. Bichsel, F. Lévy, and H. Berger, J. Phys. C: Solid State Phys., **18**, 6063-6074 (1985).

<sup>2</sup> W. Li, C.F.J. Walther, A. Kuc, and T. Heine, J. Chem. Theory Comput., **9**, 29502958 (2013).

<sup>3</sup> A. Kuc, N. Zibouche, and T. Heine, Phys. Rev. B, **83(24)**, 245213 (2011).

<sup>4</sup> A. Togo, and I. Tanaka, Scr. Mater., **108**, 1-5 (2015).